Two photon background for Higgs boson searches at the LHC

T. Binoth
Laboratoire d'Annecy-le-Vieux de Physique Théorique LAPTH

The search for an intermediate mass Higgs boson at the LHC needs the quantitative understanding of the two-photon background. A calculation of two-photon production in hadronic collisions at full next-to-leading order is described. It includes photons originating from the hadronization of QCD partons which play an important role at the LHC. A prediction for the invariant mass distribution for photon pairs at the LHC is presented and finally the residual scale dependencies are discussed.

1 Introduction

The understanding of electroweak symmetry breaking is a major motivation for present and future collider physics. Inside the Standard Model (SM) the LHC is expected to detect the predicted Higgs boson, if its mass is below say 800 GeV. On one hand the direct search at the LEP experiments place a stringent lower bound whereas on the other hand the precision measurements indicate an upper bound for the mass of the Higgs boson [1]:

$$107.7\,\mathrm{GeV} < M_{Higgs} < 188\,\mathrm{GeV} \qquad (95\%\ \mathrm{c.l.}) \tag{1}$$

Also for the light Higgs boson of the minimal supersymmetric standard model a lower bound of 88 GeV exists, where on the contrary the upper bound of around 130 GeV is dictated by the structure of the interaction terms. The quartic couplings are related to the gauge couplings here, not a free parameter as in the SM. The most promising signal for such neutral Higgs bosons in the mass range of $80\,\mathrm{GeV} < M_{Higgs} < 140\,\mathrm{GeV}$ comes from the gluon fusion process with a subsequent decay of the Higgs boson into a photon pair. Though the branching fraction is small, $B(H \to \gamma\gamma) \sim 2 \times 10^{-3}$ in the SM, one expects a sharp peak in the invariant mass distribution of the photon pair, because of the narrow Higgs width of a few MeV. Though the signal is very sharp one is confronted with a huge background. To get a quantitative understanding of the signal to background ratio one has to know the background as best as one can.

The background can be split into three contributions:

Direct: Both photons originating from the hard partonic interaction.

Fragmentation: At least one of the photons is created in the hadronization of a QCD parton.

Meson decay: The photons are decay products of mesons like π^0, η, and so on.

Whereas the latter is essentially reducible the former are commonly called irreducible backgrounds though one can reduce the fragmentation contribution substantially by imposing isolation criteria, i.e. one restricts the hadronic energy inside a cone (defined in rapidity and azimuthal angle space) around the photon momentum to be less than some value.

In the following the calculation of this background at full next-to-leading order is shortly sketched. The inclusion of the NLO fragmentation contributions is a step beyond the calculations of [2,3,4]. A prediction of the background $M_{\gamma\gamma}$ distribution at LHC is presented and its stability under variation of the different scales entering the computation is discussed.

2 Photon pair production in hadronic collisions at NLO

The Born term for photon pair production, $q\bar{q} \to \gamma\gamma$, is of order α^2. The radiative corrections consist out of all virtual and real emission corrections which lead to an order $\alpha^2\alpha_s$ correction. One observes that in subprocesses like $qg \to \gamma\gamma q$ a final state singularity is present if the photon is collinear to the quark. To absorb these singularities into a photon fragmentation function $D_{\gamma/q}$ one has subsequently also to take into account other partonic reactions like e.g. $qg \to \gamma q$. As $D_{\gamma/q}$ behaves like α/α_s in the investigated kinematic regime, the power counting of the couplings is the same as the one of the Born term. As both photons can be collinear to external partons also both photons should be allowed to be created in hadronization. Two–fragmentation processes are needed for consistency together with the respective higher order corrections, see [5] for more details. Finally there is another sizable contribution, $gg \to \gamma\gamma$, where the gluons/photons are attached to a fermion loop. Formally a higher order correction, this contribution is not negligible due to the large gluon flux at the LHC.
The diagrammatic calculation depends on three unphysical scales:

μ**:** Renormalization scale due to ultraviolet divergence,

μ_{FACT}**:** Factorization scale due to QCD initial state collinear singularities,

μ_{FRAG}**:** Fragmentation scale due to final state collinear singularities.

The relation between the hadronic and the partonic cross sections for a fragmentation process is done by folding the partonic cross sections with the μ_{FACT}-dependent parton distribution functions and the μ_{FRAG}-dependent photon fragmentation functions $D_{\gamma/j\in\{q,\bar{q},g\}}$.

3 The $M_{\gamma\gamma}$ distribution at the LHC

The comparison of our calculation with recent Tevatron data is showing a good agreement [5]. This is especially true for infrared save quantities as the $M_{\gamma\gamma}$ distribution [a]. In Fig. 1 we plot the invariant mass distribution of a photon pair at the LHC with and without applying isolation cuts. As an example we demand the transversal hadronic energy to be less than $E_{Tmax} = 5$ GeV in a cone $R = 0.4$ around the photon defined in rapidity and azimuthal angle space through $R = \sqrt{(y - y_\gamma)^2 + (\phi - \phi_\gamma)^2}$. Apart from these, standard cuts were taken as indicated in the figure. The scale choice is $\mu = \mu_{FACT} = \mu_{FRAG} = M_{\gamma\gamma}/2$. For all figures the MRST2 set of parton distribution functions [6] and the BFG photon fragmentation functions [7] were used. To get an idea of the residual scheme dependence of our result for the lower curve in Fig. 1 (with isolation), we varied the renormalization and factorization scales and compared to that curve by plotting $[d\sigma/dM_{\gamma\gamma}(\mu, \mu_{FACT}) - d\sigma/dM_{\gamma\gamma}(M_{\gamma\gamma}/2, M_{\gamma\gamma}/2)]/[d\sigma/dM_{\gamma\gamma}(M_{\gamma\gamma}/2, M_{\gamma\gamma}/2)]$ in Fig. 2. Due to isolation the fragmentation scale dependence is marginal [b] and is kept equal to μ_{FACT} for simplicity. In Fig. 2 one observes that there is an accidental stability if μ, μ_{FACT} are changed in the same directions from $\mu = \mu_{FACT} = M_{\gamma\gamma}/2$ to $\mu = \mu_{FACT} = 2M_{\gamma\gamma}$. This is due to the

[a] Infrared sensitive observables are showing also good agreement for the tails of the distributions. In the infrared sensitive region resummation of large logarithms is needed [4].

[b] This is because we consider the fragmentation contributions in the calculation. Thus the result is of beyond leading logarithmic accuracy.

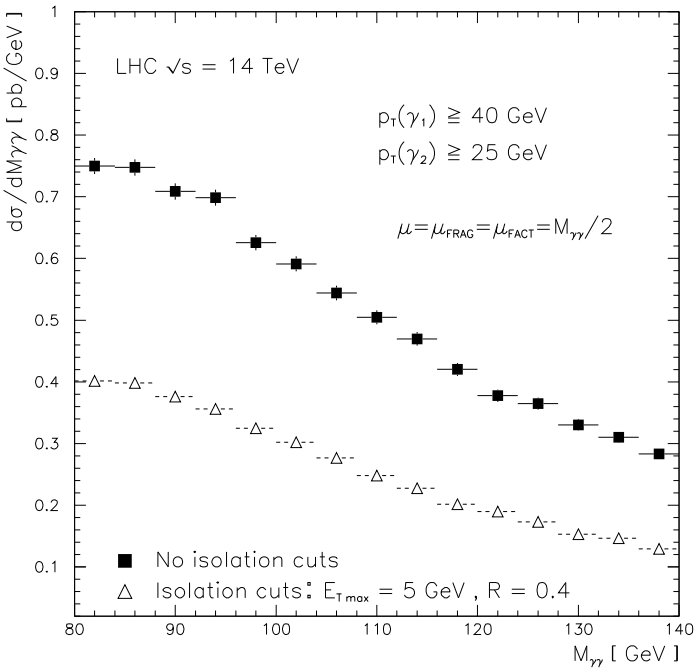

Figure 1: The $M_{\gamma\gamma}$ distribution at the LHC in the window relevant for Higgs searches using standard cuts. Applying no photon isolation criterion leads to the upper curve whereas the lower curve shows the effect of isolation. Whereas in the upper curve the one-fragmentation contribution is dominant, in the lower curve mainly the direct component is present.

fact that at LHC for the given parton energies the effect of larger (smaller) μ – means smaller (larger) NLO corrections – is compensated by the increased (decreased) gluon flux if μ_{FRAG} is also increased (decreased). By varying in an anti-diagonal way one gets a more conservative estimation of the uncertainty. One observes variations between 10 and 20 per cent.

4 Conclusion

A calculation for the photon pair production at hadron colliders at full NLO exists and is implemented into a partonic event generator, called DIPHOX[5]. Tevatron data are well described by the code and predictions for the LHC show a residual scale dependence of the order of 10 to 20 per cent [c]. For infrared sensitive observables, like e.g. P_T distributions, resummation has to be included in the calculation. In contrary the $M_{\gamma\gamma}$ distribution is now known at NLO not only in the direct but also in the fragmentation part which allows more reliable quantitative studies of effects due to isolation criteria.

Acknowledgments

I would like to thank my collaborators J. Ph. Guillet, E. Pilon and M. Werlen for giving me the opportunity to present our results at the Moriond conference.
This work was supported by the EU Fourth Training Programme "Training and Mobility of

[c] To get a further stabilization at least the dominant processes would have to be calculated one order higher. E.g. the corrections to the box contribution have to be included but also the corrections to the gluon induced subprocesses.

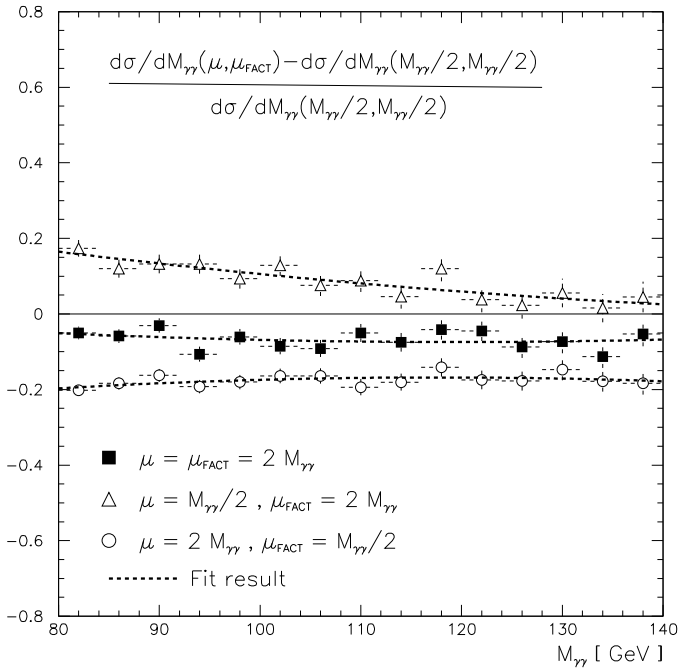

Figure 2: The behaviour of the lower curve of Fig. 1 under scale variations. The relative difference is plotted for diagonal and anti-diagonal variations of μ and μ_{FACT}. The fragmentation scale is chosen as $\mu_{FRAG} = \mu_{FACT}$.

Researchers", Network "Quantum Chromodynamics and the Deep Structure of Elementary Particles", contract FMRX–CT98–0194 (DG 12 - MIHT).

References

1. S. Muijs, Talk at the XXXVth Rencontres de Moriond.
2. P. Aurenche, R. Baier, A. Douiri, M. Fontannaz and D. Schiff, Z. Phys. **C29** (1985) 459;
   P. Aurenche, M. Bonesini, L. Camilleri, M. Fontannaz and M. Werlen, Proceedings of LHC Aachen Workshop CERN-90-10 G. Jarlskog and D. Rein eds., vol. II, p. 83.
3. B. Bailey, J. Ohnemus and J.F. Owens, Phys. Rev. **D46** (1992) 2018;
   B. Bailey and J.F. Owens, Phys. Rev. **D47** (1993) 2735;
   B. Bailey and D. Graudenz, Phys. Rev. **D49** (1994) 1486.
4. C. Balazs, E.L. Berger, S. Mrenna and C.P. Yuan, Phys. Rev. **D57** (1998) 6934;
   C. Balazs and C.P. Yuan, Phys. Rev. **D59** (1999) 114007.
5. T. Binoth, J. P. Guillet, E. Pilon, M. Werlen,
   hep-ph/9911340, to appear in The European Physical Journal C.
6. A.D. Martin, R.G. Roberts, W.J. Stirling and R.S. Thorne, hep-ph/9907231.
7. L. Bourhis, M. Fontannaz and J.Ph. Guillet, Eur. Phys. J. **C2** (1998) 529.